PHYSICAL REVIEW C **78**, 034315 (2008)

# Disappearance of the $N = 14$ shell gap in the carbon isotopic chain

M. Stanoiu,[1,2,3] D. Sohler,[4] O. Sorlin,[2] F. Azaiez,[1] Zs. Dombrádi,[4] B. A. Brown,[5] M. Belleguic,[1] C. Borcea,[3] C. Bourgeois,[1] Z. Dlouhy,[6] Z. Elekes,[4] Zs. Fülöp,[4] S. Grévy,[2] D. Guillemaud-Mueller,[1] F. Ibrahim,[1] A. Kerek,[7] A. Krasznahorkay,[4] M. Lewitowicz,[2] S. M. Lukyanov,[8] S. Mandal,[9] J. Mrázek,[6] F. Negoita,[3] Yu.-E. Penionzhkevich,[8] Zs. Podolyák,[10] P. Roussel-Chomaz,[11] M. G. Saint-Laurent,[2] H. Savajols,[2] G. Sletten,[12] J. Timár,[4] C. Timis,[3] and A. Yamamoto[10]

[1]*Institut de Physique Nucléaire, IN2P3-CNRS, F-91406 Orsay Cedex, France*

[2]*Grand Accélérateur National d'Ions Lours (GANIL), CEA/DSM-CNRS/IN2P3, B. P. 55027, F-14076 Caen Cedex 5, France*

[3]*IFIN-HH, P. O. Box MG-6, 76900 Bucharest-Magurele, Romania*

[4]*Institute of Nuclear Research of the Hungarian Academy of Sciences, P. O. Box 51, H-4001 Debrecen, Hungary*

[5]*National Superconducting Cyclotron Laboratory, Michigan State University, East Lansing, Michigan 48824, USA*

[6]*Nuclear Physics Institute, AS CR, CZ 25068, Rez, Czech Republic*

[7]*Royal Institute of Technology, Stockholm, Sweden*

[8]*FLNR, JINR, RU-141980 Dubna, Moscow region, Russia*

[9]*Laboratoire de Physique Corpusculaire, 14000 Caen Cedex, France Caen, 14021, France*

[10]*Department of Physics, University of Surrey, Guildford, GU2 5XH, United Kingdom*

[11]*Grand Accélérateur National d'Ions Lourds (GANIL), CEA/DSM-CNRS/IN2P3, B. P. 55027, F-14076 Caen Cedex 5, France*

[12]*Niels Bohr Institute, University of Copenhagen, Denmark*

(Received 5 June 2008; published 23 September 2008)

The structure of ${}^{17-20}_{\ \ \ 6}$C nuclei was investigated by means of the in-beam $\gamma$-ray spectroscopy technique using fragmentation reactions of radioactive beams. Based on particle-$\gamma$ and particle-$\gamma\gamma$ coincidence data, level schemes are constructed for the neutron-rich $^{17-20}$C nuclei. The systematics of the first excited $2^+$ states in the carbon isotopes is extended for the first time to $A = 20$ showing that in contrast to the case of the oxygen isotopes, the $N = 14$ subshell closure disappears. Experimental results are compared with shell-model calculations. Agreement between them is found only if a reduced neutron-neutron effective interaction is used. Implications of this reduced interaction in some properties of weakly bound neutron-rich Carbon are discussed.

DOI: 10.1103/PhysRevC.78.034315 PACS number(s): 23.20.Lv, 21.60.Cs, 25.70.Mn, 27.20.+n

## I. INTRODUCTION

The formation of nuclear shell gaps, as well as their collapse in certain regions of the chart of nuclides, is largely being investigated worldwide. It affects many unique features in nuclear physics as the abundance of the stable elements in the universe, the possible existence of an island of super heavy nuclei, the route of heavy nuclei to fission and the existence of cluster configurations.

It is a remarkable fact that the shell (or subshell) gaps, such as 14, 28, 50, and, to a weaker extent, 82 and 126, share a common origin. Taking, for instance, the neutron shell gaps, they are formed by the combined action of the spin-orbit (SO) force and by neutron-neutron interactions. The former force significantly binds the orbit in which the angular momentum and intrinsic spin are aligned (denoted as $\ell_\uparrow$). In addition, the filling of neutrons inside this orbit amplifies its binding due to the attractive neutron-neutron $V^{nn}_{\ell_\uparrow\ell_\uparrow}$ force of mainly pairing origin. As an example, the $N = 28$ shell gap is formed by the action of the SO force on the $f$ orbit, which splits the aligned $f_{7/2}$ ($\ell_\uparrow$) and antialigned $f_{5/2}$ ($\ell_\downarrow$) components by about 6 MeV apart in $^{40}$Ca. It pushes down the $f_{7/2}$ single-particle state below the $p_{3/2}$ one, creating a small $N = 28$ gap of about 2 MeV between these two orbits. Going from $^{40}$Ca to $^{48}$Ca, 8 neutrons have filled the $f_{7/2}$ orbit. This increases (decreases) the binding of the $f_{7/2}$ ($p_{3/2}$) orbit due to the action of attractive (repulsive) neutron-neutron forces. Consequently the $N = 28$ gap grows up to reach about 4.9 MeV in $^{48}$Ca, making this nucleus doubly magic. Despite the fact that the mechanism to create shell gaps by means of attractive neutron-neutron two-body matrix elements (TBME) $V^{nn}$ is well understood, the size of the empirical value required (here $V^{nn}_{f_{7/2}f_{7/2}}$) cannot be derived from realistic interactions between free nucleons. This points to the need for three-body forces [1], the intensities of which should be constrained by experimental data at these major shell closures.

Another effect that plays a role in increasing or decreasing the above-mentioned shell gaps is the proton-neutron tensor interaction. An example can be found in the significant reduction of the $N = 28$ shell gap when one goes from Ca down to Si [2,3]. While removing protons from the $d_{3/2}$ orbit between Ca to S, the strongly attractive force $V^{pn}_{d_{3/2}f_{7/2}}$ is no longer present [4]. This makes the neutron $f_{7/2}$ less bound and reduces the size of the $N = 28$ gap by about 1.1 MeV between $^{40}$Ca and $^{34}$Si.

In addition, as one approaches the neutron drip line, the dependence of orbital energy on $\ell$ [5] becomes important. As an example, the Skx Skyrme interaction [6] (without SO) gives single-particle energies of −6.16 (−5.66) MeV for the $0f$ ($1p$) orbit in $^{48}$Ca compared to −1.03 (−1.57) MeV in $^{42}$Si. In this simple approach the $p$ states becomes more bound than the $f$ one in $^{42}$Si. The lowering in energy of the low-$\ell$ orbits relative to high $\ell$ is a consequence of the loose binding in a finite-well potential. Thus, the shell gaps are due to a combination of several factors that depend on the orbits being filled and distance to stability.

These competing effects of the nuclear force, described for $N = 28$, should to some extent be encountered for other shell gaps that share a common origin, such as $14, 50 \ldots$. In this context the recent discovery of the $N = 14$ shell gap of about 4 MeV in the oxygen chain [7,8] provides an ideal opportunity to study these facets of the nuclear force. This can be done by studying neutron-rich C isotopes around $N = 14$. In addition, it has been deduced from studies of the neutron-rich light B [9,10] and N [11] nuclei that a significant reduction of the monopole part of the neutron-neutron matrix elements has to be applied to account for their spectroscopic properties. If a similar reduction of the $V^{nn}$ has to be applied for the C chain, the strength of the $N = 14$ gap would be further reduced.

The present work focuses on the spectroscopy of the neutron-rich C isotopes, among which $^{20}C_{14}$ is studied for the first time (preliminary results were presented in Ref. [12]). A comparison of the structural evolution between the O and C chains follows, aiming at searching for a possible reduction of the $N = 14$ shell gap.

## II. EXPERIMENTAL METHODS

The excited states of the heaviest C isotopes were studied using the in-flight double step fragmentation reaction, the basic details of which were given in Ref. [7]. A beam of $^{36}$S (with an average intensity of 400 pnA) was accelerated to an energy of 77.5 MeV per nucleon by two cyclotrons of the GANIL facility to induce fragmentation reactions into a 398-mg/cm$^2$-thick C target placed inside the SISSI device. Projectile-like fragments of interest were selected through the $\alpha$ spectrometer. A wedge-shaped, 130-mg/cm$^2$-thick, Al foil was installed at the dispersive focal plane between the two dipoles of the spectrometer to provide an additional energy-loss selection. The magnetic rigidity of the $\alpha$ spectrometer was optimized for the transmission of a secondary beam cocktail composed of $^{24}$F, $^{25,26}$Ne, $^{27,28}$Na, and $^{29,30}$Mg nuclei with energies varying from 54 MeV per nucleon up to 65 MeV per nucleon. An "active" target composed of a plastic scintillator (103.5 mg/cm$^2$) sandwiched between two carbon foils of 51 mg/cm$^2$ was used both for identifying the nuclei of the cocktail beam through their time-of-flight values and for inducing secondary reactions. The secondary fragments were subsequently selected and identified through the SPEG spectrometer using time-of-flight, energy loss, and focal-plane position information.

The "active" target was surrounded by a $\gamma$-detector array of 74 $BaF_2$ detectors placed at a mean distance of 30 cm from the target to detect the prompt $\gamma$ decay of the secondary fragments. The relatively high velocity of the produced projectile fragments ($v/c \simeq 0.35$) requires the application of Doppler shift corrections to the energy of the detected $\gamma$ rays. The total photopeak efficiency of the $BaF_2$ array was 30% for a $\gamma$ ray of 1.3 MeV. The energy resolution (FWHM), including the part provided by the Doppler broadening, amounts to 15%. Low-energy $\gamma$ transitions down to 100 keV were detected with an efficiency value of about 24%.

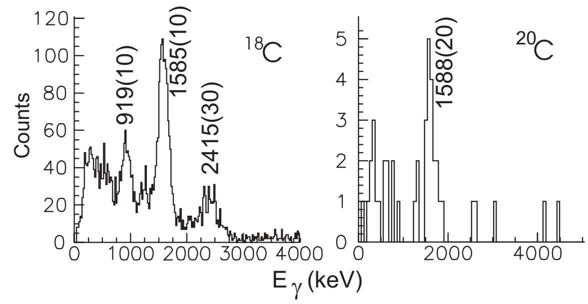


FIG. 1. $\gamma$-ray spectrum of $^{18}$C and $^{20}$C.

## III. RESULTS AND DISCUSSION

The Doppler-corrected $\gamma$ spectra observed for $^{18}$C and $^{20}$C are shown in Fig. 1. The first excited state in $^{18}$C has been proposed to be at 1620(20) keV [13]. This corresponds, very likely, to the 1585(10)-keV transition observed with the highest intensity in the present work. Two additional $\gamma$ lines were observed at 919(10) and 2415(30) keV (see Fig. 1). By exploiting the $\gamma$-$\gamma$ coincidences, it is deduced that the 919- and 2415-keV transitions are in coincidence with the 1585-keV one but not in mutual coincidence. The proposed level scheme of $^{18}$C (Fig. 2) is based on these pieces of information.

Prior to the present work, information on the $^{20}$C nucleus was limited to lifetime and atomic mass values. Even if produced at a low rate of 4/h using this double step fragmentation method, the $\gamma$-ray spectrum clearly exhibits a peak at 1588(20) keV (see Fig. 1). This unique $\gamma$ line is assigned to the $2^+ \to 0^+$ transition, placing for the first time the energy of the first $2^+$ state of $^{20}$C at 1588(20) keV.

The $\gamma$-ray spectrum of the odd nucleus $^{17}$C exhibits two transitions (see Fig. 3). Their relative intensity is the same in the $\gamma$-ray spectra of $^{17}$C obtained from the low and high $\gamma$-ray multiplicity events. This indicates that both transitions correspond to the decay of two excited states at 207 and 329 keV directly to the ground state. Additional pieces of information exist from other experimental works. The $^{17}$C ground state has a $3/2^+$ spin value [14]. A level at about 300 keV has been evidenced from transfer reaction experiments [15,16]. Given the typical energy resolution obtained there, this level could be a mixture of the two states observed in our experiment. The neutron knock-out experiment performed at RIKEN [17] is in accordance with our results with two

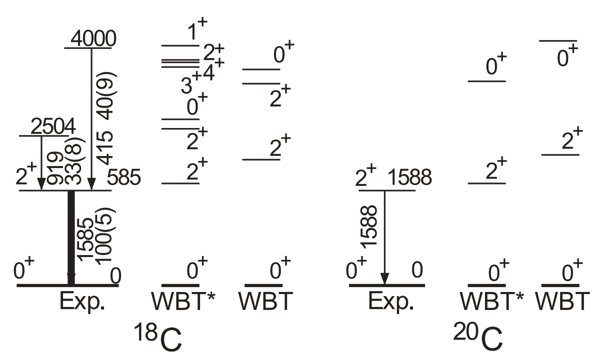


FIG. 2. Level scheme of $^{18}$C and $^{20}$C in comparison with shell-model calculations with the WBT* and WBT interactions.

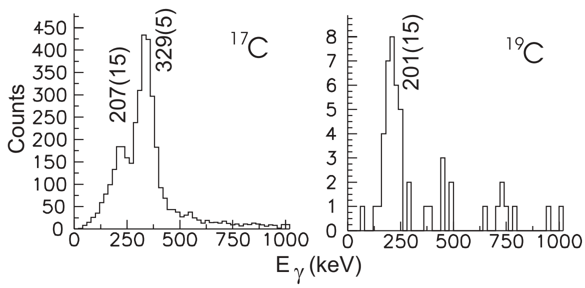


FIG. 3. $\gamma$-ray spectra of $^{17}$C and $^{19}$C obtained in the present experiment.

excited states at 210(4) and 331(6) keV. From the $^{17}$C$(p, p')$ study a tentative spin $1/2^+$ was assigned to the lower energy state and a spin $5/2^+$ to the higher energy one [17]. Gathering all experimental works, a level scheme is proposed. It is in accordance with shell-model calculations [18], the accuracy of which could not be better than a few hundred keV.

For $^{19}$C, one-neutron break-up reactions proposed a $1/2^+$ configuration for the ground state [19]. As the 201-keV $\gamma$ transition is observed in our work as a prompt radiation, it should connect states separated by small spin differences such as $3/2^+ \rightarrow 1/2^+$ or $3/2^+ \rightarrow 5/2^+$. A stretched $E2$ transition of 201 keV, connecting, for instance, $5/2^+$ and $1/2^+$ states, would have a half-life of the order of a $\mu s$. By means of the $^{19}$C$(p, p')$ reaction, two $\gamma$-ray transitions with energies of 197(6) keV and 72(4) keV were assigned to $^{19}$C [17]. The authors placed these two $\gamma$ rays in cascade, the 197 keV one having the lowest energy. Similarly to $^{17}$C [18], shell-model calculations predict the existence of three low-lying states with spins $1/2^+, 3/2^+$, and $5/2^+$ within a few hundred keV (see Fig. 4).

The present results extend the systematics of the $2^+$ excitation energy up to $N = 14$ in the carbon isotopic chain, as shown in Fig. 5. The similarity of the trend of $2^+$ energies of the C and O isotopes up to $N = 12$ is striking. A strong change appears at $N = 14$, where the $2^+$ energy of $^{20}$C is about a factor of 2 lower than for $^{22}$O [7].

This different behavior between the O and C chains is a consequence of the crossing of the neutron $s_{1/2}$ and $d_{5/2}$ orbits that arises between the $^{17}$O and $^{15}$C isotones. From their level schemes, it can be derived that the $s_{1/2}$ neutron single-particle energy decreases relative to the $d_{5/2}$ one by 1.6 MeV, whereas two protons are removed from the $p_{1/2}$

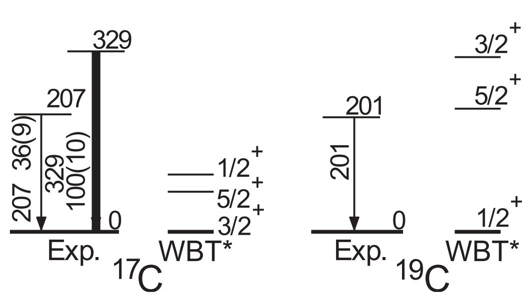


FIG. 4. Level schemes of $^{17}$C and $^{19}$C as observed in the present experiment and their comparison with shell-model calculations using the WBT* interaction.

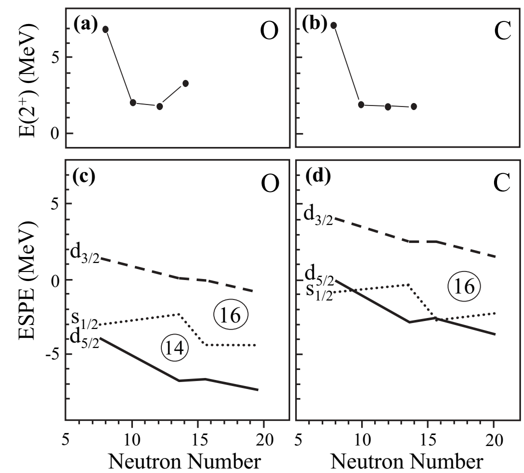


FIG. 5. (a) Evolution of the $2^+$ energies as a function of the neutron number in oxygen and (b) carbon nuclei. Evolution of effective single-particle energies (ESPE) as a function of the neutron number calculated by using the USD effective interaction for the (c) oxygen and (d) carbon isotopes. The ESPE evolution is derived from the WBT interaction. The use of the WBT* one would lead to a further compression of ESPE.

orbit, giving rise to a $1/2^+$ for the $^{15}$C ground state [20]. This inversion of levels owes to the difference of proton-neutron TBME, $2(V^{pn}_{p_{1/2}d_{5/2}} - V^{pn}_{p_{1/2}s_{1/2}})$. The first monopole contains an attractive tensor term, whereas the second one has a repulsive two-body LS term [21]. In addition, we expect some shift from the finite potential well of the central interaction. For instance, the Skx Skyrme interaction [6] (without spin-orbit) gives single-particle energies of $-3.44$ ($-3.76$) MeV for the $0d$ ($1s$) orbit in $^{16}$O compared to $+0.48$ ($-0.97$) MeV in $^{14}$C, i.e., a relative change of 1.13 MeV between the $d$ and $s$ orbits.

The evolution of the $s_{1/2}$ and $d_{5/2}$ effective single-particle energies (ESPE) in the O and C chains as a function of the neutron number is shown in Fig. 5. Starting from $^{17}$O, the addition of five neutrons in the $d_{5/2}$ orbit leads to a gradual gain of its energy with respect to the $s_{1/2}$ by virtue of the large attractive $V^{nn}_{d_{5/2}d_{5/2}}$ matrix element. This gives rise to a new gap at $N = 14$ between the $d_{5/2}$ and $s_{1/2}$ orbits of about 4.2 MeV [7]. This large gap accounts for the high energy of the $2^+_1$ state in $^{22}$O$_{14}$ that has a $[(d_{5/2})^5, s_{1/2}]$ configuration. At $N = 15$ the $s_{1/2}$ orbit starts to fill, with a quasi-pure single-particle configuration [22]. A large $N = 16$ gap of more than 4 MeV is also present between the $s_{1/2}$ and $d_{3/2}$ orbits at $N = 16$ [22,23]. For the O isotopes WBT uses the USD Hamiltonian [24] for the $sd$ shell. The more recent USDA/B Hamiltonians [25] differ from USD mainly for the $d_{3/2}$ orbit between $N = 16$ and $N = 20$, which is about 1 MeV more bound with USD compared to USDA/B.

Adding neutrons to $^{15}$C leads to a more complicated situation. Initially the $s_{1/2}$ orbit is lower, but due to the effect described in the previous paragraph, the ESPE for $d_{5/2}$ crosses that of the $s_{1/2}$ orbit and stays close to it between $N = 8$ and $N = 14$. Therefore the configuration mixing is large and the ground state as well as the $2^+_1$ state in $^{16,18,20}$C are dominated by $(d_{5/2}, s_{1/2})^{2,4,6}$ configurations. This explains the almost constancy of the $2^+$ energies up to $^{20}$C and disappearance of the gap at $N = 14$. For $^{22}$C the $2^+$ state is expected at a higher excitation energy due to the large gap at $N = 16$. The quasidegeneracy of the $1/2^+$, $3/2^+$, and $5/2^+$ states in $^{17}$C and $^{19}$C is related to the close spacing between $s_{1/2}$ and $d_{5/2}$ single-particle energies. This situation also leads to the possibility of many halo configurations in the carbon isotopes related to the loosely bound $s_{1/2}$ orbital.

The experimental level schemes of $^{18,20}$C (Fig. 2) are compared to shell-model calculations using the WBT [18] interaction. This interaction uses the USD TBME that reproduced the level energies of the heavy O nuclei successfully [7]. However, the experimental spectra for the C isotopes are systematically compressed compared to the calculations. Similar results of ESPE and $2_1^+$ excitation energies of $^{18}$C and $^{20}$C were found by Suzuki *et al.* [26], who used a Hamiltonian with enhanced tensor interaction and corrections in the $T = 1$ monopole terms. Empirically, if the neutron-neutron TBME of WBT are multiplied by 0.75, the spectra are in better agreement with experiment (the results labeled WBT* in the figure). This observation is in accordance with the fact that some properties of neighboring nuclei, such as binding energies, magnetic moments, and spectroscopy [9,10,27,28], could be better described by means of a reduced strength of the neutron-neutron TBME as well.

The fundamental source of this reduction needs to be understood. There are at least two possibilities. One is that neutron *sd* shell orbits are more loosely bound in the C isotopes. For example, the $s_{1/2}$ state is bound by 1.2 MeV in $^{14,15}$C compared to 3.3 MeV in $^{16,17}$O. The measured root-mean-square matter radii of the weakly bound C are systematically larger than in the O isotones [29], which can be due to the weakly bound valence neutrons [30]. Calculations with a $\delta$-function form for the interaction show that this can lead to up to a 20% reduction in the TBME involving the $s_{1/2}$ orbit. Another factor is that the core-polarization contributions can change. For the O isotopes part of it is due to the excitation of the $p_{1/2}$ protons into the *sd* and higher shells. For the C isotopes the $p_{1/2}$ proton orbit is nearly empty and cannot contribute to the core polarization. Quantitative calculations of these effects remain to be done.

## IV. CONCLUSION

The spectroscopy of C isotopes up to $^{20}$C has been carried out for the first time. From the systematics of the $2_1^+$ energies, it is found that the $N = 14$ subshell gap is no longer present in the C isotopic chain. This sudden breakdown is both ascribed to the early crossing of the $s_{1/2}$ and $d_{5/2}$ levels at $N = 9$ due to reduced proton-neutron tensor forces, the finite-well potential, and to the reduced neutron-neutron interaction when going from O to C nuclei. Reasons for the reduction of $V^{nn}$ have been proposed, but they should be ascertained with further theoretical and experimental studies. The present study on the $N = 14$ shell closure shows a strong analogy with earlier findings at $N = 28$, revealing that a generic mechanism acts to destroy the "major" shell closures. Applied to the next shell closure $N = 50$, the $^{78}\mathrm{Ni}_{50}$ could turn out to be *not* doubly magic. For heavier nuclei, the stronger spin-orbit force acting on large $\ell$ values keeps the magicity for the $N = 82$ and $N = 126$ shell closures, i.e., for $^{132}$Sn and $^{208}$Pb.

## ACKNOWLEDGMENTS

This work has been supported by the European Community contract No. RII3-CT-2004-506065, by OTKA K68801 and by NSF PHY-0555366 grants. The GANIL technical staff as well as S. Franchoo are greatly acknowledged.

[1] E. Caurier *et al.*, Rev. Mod. Phys. **77**, 427 (2005).
[2] B. Bastin *et al.*, Phys. Rev. Lett. **99**, 022503 (2007).
[3] C. M. Campbell *et al.*, Phys. Rev. Lett. **97**, 112501 (2006).
[4] L. Gaudefroy *et al.*, Phys. Rev. Lett. **97**, 092501 (2006).
[5] I. Hamamoto, Phys. Rev. C **76**, 054319 (2007).
[6] B. A. Brown, Phys. Rev. C **58**, 220 (1998).
[7] M. Stanoiu *et al.*, Phys. Rev. C **69**, 034312 (2004); M. Stanoiu, PhD Thesis, GANIL T 03 01 (2003).
[8] A. Schiller *et al.*, Phys. Rev. Lett. **99**, 112501 (2007).
[9] M. Stanoiu *et al.*, Eur. Phys. J. A **22**, 5 (2004).
[10] Zs. Dombrádi *et al.*, Phys. Lett. **B621**, 81 (2005).
[11] D. Sohler *et al.*, Phys. Rev. C **77**, 044303 (2008).
[12] M. Stanoiu *et al.*, Eur. Phys. J. A **20**, 95 (2004); Nucl. Phys. **A746**, 135c (2004).
[13] L. K. Fifield *et al.*, Nucl. Phys. **A385**, 505 (1982).
[14] E. Sauvan *et al.*, Phys. Lett. **B491**, 1 (2000).
[15] J. A. Nolen *et al.*, Phys. Lett. **B71**, 314 (1977); K. Fifield *et al.*, Nucl. Phys. **A385**, 505 (1982).
[16] H. G. Bohlen *et al.*, Eur. Phys. J. A **31**, 279 (2007).
[17] Z. Elekes *et al.*, Phys. Lett. **B614**, 174 (2005).
[18] E. K. Warburton and B. A. Brown, Phys. Rev. C **46**, 923 (1992).
[19] V. Maddalena *et al.*, Phys. Rev. C **63**, 024613 (2001).
[20] I. Talmi and I. Unna, Phys. Rev. Lett. **4**, 469 (1960).
[21] T. Otsuka (private communication).
[22] Z. Elekes *et al.*, Phys. Rev. Lett. **98**, 102502 (2007).
[23] C. R. Hoffman *et al.*, Phys. Rev. Lett. **100**, 152502 (2008).
[24] B. A. Brown and B. H. Wildenthal, Annu. Rev. Nucl. Part. Sci. **38**, 29 (1988).
[25] B. A. Brown and W. A. Richter, Phys. Rev. C **74**, 034315 (2006).
[26] T. Suzuki , R. Fujimoto, and T. Otsuka, Phys. Rev. C **67**, 044302 (2003).
[27] D. Bazin *et al.*, Phys. Rev. Lett. **74**, 3569 (1995).
[28] H. Ueno *et al.*, Phys. Rev. C **53**, 2142 (1996).
[29] A. Ozawa *et al.*, Nucl. Phys. **A693**, 32 (2001).
[30] B. A. Brown, S. Typel, and W. A. Richter, Phys. Rev. C **65**, 014612 (2001).